

Modeling the desired direction in a force-based model for pedestrian dynamics

Mohcine Chraïbi^{1,2}, Martina Freialdenhoven¹, Andreas Schadschneider³, and Armin Seyfried^{1,2}

¹ Jülich Supercomputing Centre, Forschungszentrum Jülich. 52425 Jülich, Germany.

m.chraibi@fz-juelich.de

MartinaFreialdenhoven@web.de

a.seyfried@fz-juelich.de

² Computer Simulation for Fire Safety and Pedestrian Traffic, Bergische Universität Wuppertal, Pauluskirchstraße 11, D-42285 Wuppertal, Germany.

³ Institute for Theoretical Physics, Universität zu Köln, D-50937 Köln, Germany. as@thp.uni-koeln.de

Summary. We introduce an enhanced model based on the generalized centrifugal force model. Furthermore, the desired direction of pedestrians is investigated. A new approach leaning on the well-known concept of static and dynamic floor-fields in cellular automata is presented. Numerical results of the model are presented and compared with empirical data.

Force-based models try to describe the dynamics of pedestrians as reaction to forces acting on each single pedestrian. Basically two kinds of forces can be distinguished:

- *driving forces* designed to drive pedestrians to a desired direction with a desired speed.
- *repulsive forces* which are responsible for preserving the volume exclusion of pedestrians.

Since the introduction of force-based models [1] many works were dedicated to investigations of the repulsive forces and finding new and better forms [2–6]. These efforts for improving the form of the repulsive force is understandable, since the interactions between pedestrians dominate the dynamics, especially at high densities. Surprisingly, not much work has been done on the influence of the specific form of the driving force which is expected to dominate the behavior at low or intermediate densities.

The standard form of the driving force is

$$\vec{F}_i^{\text{drv}} = m_i \frac{\vec{v}_i^0 - \vec{v}_i}{\tau}, \quad (1)$$

with a relaxation time τ and a desired velocity \vec{v}_i^0 . Although this expression is simple, it is not clear how to choose the desired direction

$$\vec{e}_i^0 = \frac{\vec{v}_i^0}{\|\vec{v}_i^0\|} \quad (2)$$

in a given situation and only very few works were concerned with modeling the desired direction (2). In [7] an Ansatz with directing lines was introduced to steer pedestrians around 90° and 180° corners. Gloor et al. [8] used a path-oriented approach to model the desired direction of agents on given hiking paths.

In [9] Moussaïd et al. have formulated the determination of the desired direction in form of a minimization problem.

It should be mentioned that the *directing problem* we discuss here, i.e. the determination of the desired direction for each pedestrian, is conceptually different from the classical *routing problem*. In [10] an algorithm for generating automatically a navigation graph in complex buildings in combination with directing lines at corners was proposed. Another algorithm for way finding in buildings was proposed in [11]. Recently a further development of the notion of the “quickest path” using a non-iterative method to estimate the desired direction in the social force model (SFM) was introduced [12]. The main concern in this class of problems is how to define and connect intermediate targets, in order to facilitate the evacuation of pedestrians. By contrast, in the directing problem the existence of such intermediate targets is in general assumed.

In this work we introduce enhancements of the generalized centrifugal force model (GCFM) and investigate on their basis the modeling of the desired direction (2). For the sake of demonstration we test our model in two different geometries: a bottleneck and a corner.

1 The model

In this section we give a brief overview of the GCFM and its definition. Furthermore we introduce an effective modification of the pedestrian-wall interactions that simplifies the definition of the repulsive force.

1.1 Pedestrian-pedestrian repulsive interactions

Introducing the vector connecting the positions of pedestrians i and j ,

$$\vec{R}_{ij} = \vec{R}_j - \vec{R}_i, \quad \vec{e}_{ij} = \frac{\vec{R}_{ij}}{\|\vec{R}_{ij}\|}, \quad (3)$$

the repulsive force in the GCFM reads

$$\vec{F}_{ij}^{\text{rep}} = -m_i k_{ij} \frac{(\eta v_i^0 + v_{ij})^2}{d_{ij}} \vec{e}_{ij}, \quad (4)$$

with $m_i = 1$ the mass of i and the effective distance between pedestrian i and j ,

$$d_{ij} = \|\vec{R}_{ij} - r_i(v_i) - r_j(v_j)\|, \quad (5)$$

and the polar radius r_i of pedestrian i .

The relative velocity v_{ij} is defined such that slower pedestrians are less affected by the presence of faster pedestrians in front of them:

$$\begin{aligned} v_{ij} &= \frac{1}{2} [(\vec{v}_i - \vec{v}_j) \cdot \vec{e}_{ij} + |(\vec{v}_i - \vec{v}_j) \cdot \vec{e}_{ij}|] \\ &= \begin{cases} (\vec{v}_i - \vec{v}_j) \cdot \vec{e}_{ij} & \text{if } (\vec{v}_i - \vec{v}_j) \cdot \vec{e}_{ij} > 0 \\ 0 & \text{otherwise.} \end{cases} \end{aligned} \quad (6)$$

The parameter

$$\begin{aligned} k_{ij} &= \frac{1}{2} \frac{\vec{v}_i \cdot \vec{e}_{ij} + |\vec{v}_i \cdot \vec{e}_{ij}|}{v_i} \\ &= \begin{cases} (\vec{v}_i \cdot \vec{e}_{ij}) / \|\vec{v}_i\| & \text{if } \vec{v}_i \cdot \vec{e}_{ij} > 0 \text{ \& } \|\vec{v}_i\| \neq 0 \\ 0 & \text{otherwise,} \end{cases} \end{aligned} \quad (7)$$

reduces the effective range of the repulsive force to the angle of vision. Through the coefficient k_{ij} the strength of the repulsive force depends on the angle: it is maximal when pedestrian j is in the direction of motion of pedestrian i and minimal when the angle between j and i is bigger than 90° .

1.2 Wall-pedestrian repulsive interactions

In the GCFM the interactions between pedestrians and walls are modeled by a force similar to the pedestrian-pedestrian repulsive force. A wall is represented by three point masses acting on pedestrians within a certain range. From a computational point of view this analogy exhibits an overhead since the repulsive force between a pedestrian and a wall is calculated three times.

We now make use of the “distance of closest approach” as defined in [6] to formulate the repulsive force between a pedestrian i and a wall w as

$$\vec{F}_{iw}^{\text{rep}} = \eta' \|\vec{v}_i\| k_{iw} b_{iw}, \quad (8)$$

with

$$b_{iw} = H \left(1 - \frac{d_{iw}}{r+l} \right) \cdot \left(1 - \frac{d_{iw}}{r+l} \right), \quad (9)$$

where l is the distance of closest approach between an ellipse and a line, r is the polar radius determined by the nearest point on the line to the center

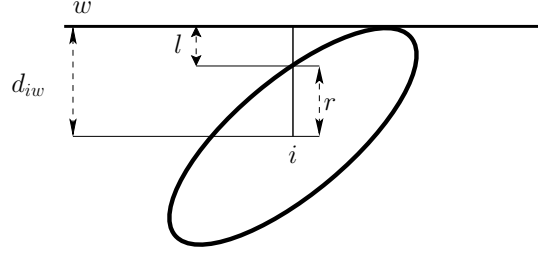


Fig. 1: Illustration of distances used in the definition of the wall-pedestrian repulsive force (8).

of the ellipse i (Fig. 1). $H()$ is the Heaviside step function, k_{iw} is defined in Eq.(7), $\|\vec{v}_i^0\|$ is the desired speed of i and η' is a parameter to control the strength of the force.

The repulsive force (8) is a contact force that is different from zero if the effective distance of the center of the ellipse to the segment line is non-positive. For the simulations in this paper we set the strength of the repulsive forces as $\eta = 0.2$ and $\eta' = 5$.

2 Influence of the desired direction

In this section we study the effects of the desired direction on the dynamics of a system by measuring the outflow from a bottleneck with different widths. See Fig. 2 for the simulation set-up. Four different methods for setting the direction of the desired velocity are introduced and discussed. Finally, simulation results will be compared.

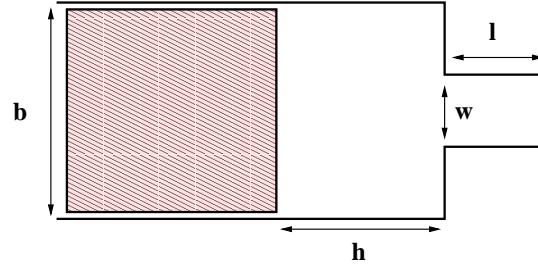


Fig. 2: Scenario set-up: Pedestrians move from a holding area (shaded region) through the bottleneck ($l = 2.8$ m, $h = 4.5$ m, $b = 4$ m and w variable).

2.1 Strategy 1: Directing towards the middle of the exit

The first strategy is probably the most obvious one. Herein, the desired direction e_i^0 for pedestrian i is permanently directed towards a reference point that exactly lies on the middle of the exit. In some situations it happens that pedestrians can not get to the chosen reference point without colliding with walls. To avoid this and to make sure that all pedestrians can “see” the middle of the exit the reference point e_1 is shifted by half the minimal shoulder length $b_{\min} = 0.2 \text{ m}$ (Fig. 3). Pedestrians that pass to the right of the reference point e_1 head towards e_2 .

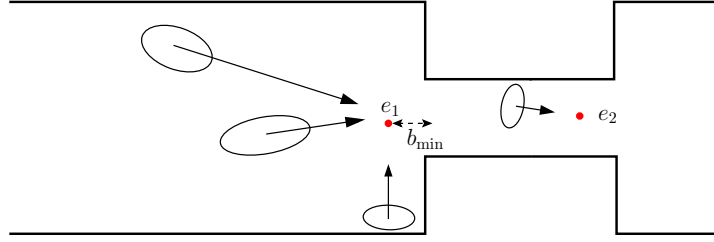


Fig. 3: Strategy 1: All pedestrians are directed exactly towards the reference points e_1 and e_2 .

2.2 Strategy 2: Enhanced directing towards the middle of the exit

This is a modification of strategy 1. Pedestrians are still directed to the shifted reference point e_1 . However, from a certain position pedestrians can see through the bottleneck the second reference point e_2 . In this case e_1 is ignored and the desired direction is set to be parallel to the line $\overrightarrow{e_1 e_2}$. Since, pedestrians that are inside the bottleneck can always see e_2 the desired direction is kept parallel to $\overrightarrow{e_1 e_2}$.

Here again the reference points and the delimiting range of the bottleneck is shifted in x - and y -direction by b_{\max} (Fig. 4).

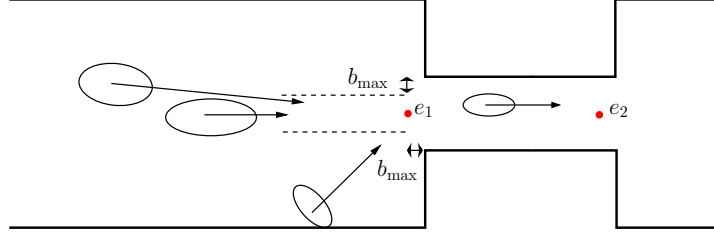


Fig. 4: Strategy 2: Depending on their position pedestrians adapt their direction. In the range where the exit of the bottleneck is visible (marked by dashed lines) the direction is longitudinal. Outside this area they are directed towards the middle of the bottleneck.

2.3 Strategy 3: Directing towards the nearest point on the exit

Another possibility to choose the desired direction \vec{e}_i^0 is to define a line l in front of the exit and take at each time the nearest point from the pedestrian i to l (Fig. 5). In comparison with strategy 2, pedestrians that are not in the range where the point e_2 is not visible choose one of the end points of the line l . In strategy 2 this would be the middle of l .

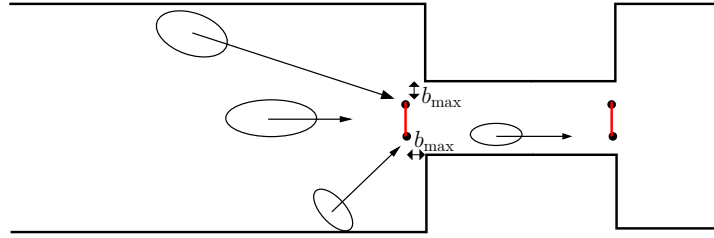


Fig. 5: Strategy 3: Directing towards the nearest point on the exit. Molnár published in [13] a very similar strategy. The only difference is the placement of the line, which is away from the corner by b_{\max} .

2.4 Strategy 4: Guiding line segments

Without loss of generality we introduce the main idea of strategy 4 with help of the previous bottleneck. Unlike the previous strategies this strategy is applicable to all geometries with corners even if the exit point is not visible. We recall that in strategy 3 a line in front of the bottleneck was defined. The nearest point from each pedestrian to this line was set to define the desired direction. As a generalization we make use in strategy 4 of three different lines to “smoothen” merging in front of the bottleneck (Fig. 6).

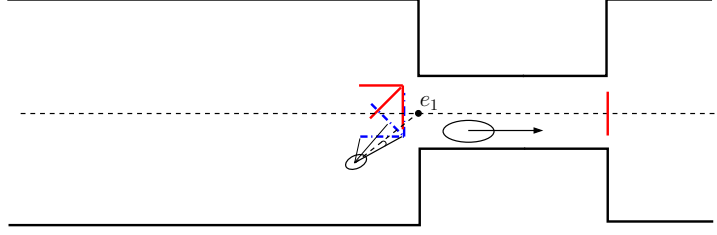


Fig. 6: Strategy 4: Guiding line segments in front of the bottleneck. For each corner a set of three line segments is generated. The length of all directing lines is equal to 3.5 m.

The blue line set (down the dashed line segment) is considered by pedestrians in the lower half and the red line set by pedestrians in the upper half of the bottleneck. For a pedestrian i at position p_i we define the angle

$$\theta_i = \arccos \left(\frac{\overrightarrow{p_i e_1} \cdot \overrightarrow{p_i l_{ij}}}{\|\overrightarrow{p_i e_1}\| \cdot \|\overrightarrow{p_i l_{ij}}\|} \right), \quad (10)$$

with l_{ij} the nearest point of the line j to the pedestrian i .

The next direction is then chosen as

$$\vec{e}_i^0 = \frac{\overrightarrow{p_i l_{ij}}}{\|\overrightarrow{p_i l_{ij}}\|} \quad (11)$$

with j such that $\theta_j = \min\{\theta_1, \theta_2, \theta_3\}$. As in strategy 3 the direction lines are shifted in x - and y -direction by b_{\min} .

2.5 Numerical results

In the previous section we have proposed different methods (called strategies) for choosing the desired direction \vec{e}_i^0 . To compare these strategies we have performed simulations for a bottleneck using the same set of parameters for the GCFM. For each strategy only the width of the bottleneck was varied from 1 m to 2.4 m.

On the basis of a quantitative analysis the importance of the choice of strategy for the observed behavior can be estimated. In the following, for each strategy we measure the flow through bottlenecks of varying width w . The flow is measured directly at the entrance of the bottleneck according to

$$J = \frac{N_{\Delta t} - 1}{\Delta t}, \quad (12)$$

with $N_{\Delta t} = 60$ pedestrians and Δt the time necessary that all pedestrians pass the measurement line.

In Fig. 7 the resulting flow for all four strategies is presented.

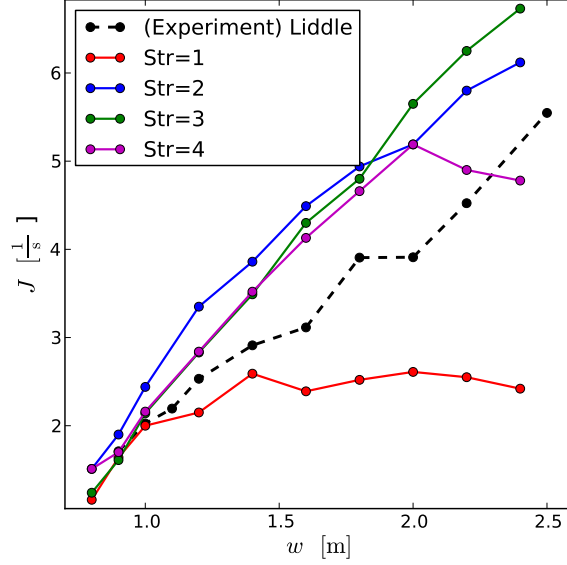


Fig. 7: Flow through a bottleneck with different widths. Simulation results with different strategies for the desired direction of pedestrians in comparison with empirical data from [14]. The experiments were conducted with 180 persons.

The flow for strategy 1 saturates independently of the width. This was expected since pedestrians do not use the whole width of the bottleneck and keep indeed oriented to the middle. The picture changes for strategies 2 – 4, where the effective width of the bottleneck is clearly larger. Strategy 2 shows a better usage of the middle widths ($\leq 1.8\text{m}$). Here, the slight blocking near the corners, that emerges from strategy 3 is particularly disadvantageous. Strategy 4 produces higher flows for widths up to 2 m. Up 2 m the flow stagnates. The main observations are:

- The choice of the strategy for the desired direction influences considerably the outcome of the simulation.
- An inconsiderate choice of strategy, in that case strategy 1, can lead to large variations from experimental results.
- In contrast to strategy 1, strategies 2 – 4 show better usage of the bottleneck width and lead to higher flow values.

3 An application: Motion around a corner

Basically, force-based models are functional only in areas, where the exit is constantly visible by all pedestrians. Obviously, this can not always be guaranteed which is a problem since a proper initialization of the desired direction \vec{e}_i^0 for each pedestrian is not possible. In order to overcome this problem one has to introduce “virtual” exits. This was showcased previously with strategy 4.

In this section, we introduce enhancements of strategy 4 and study their impact on the movement time, i.e. the time until all pedestrians have left the simulation set up. For simplicity we consider the movement of $N = 100$ pedestrians in a 90°-corner-like corridor.

The basis of our enhancements is the following observation: Given a guiding line l , the desired direction of a pedestrian i is determined in dependence of its position and the nearest point to l . This choice neglects two important factors:

1. The perception of space: Individuals try to minimize, when possible, their path to the exit. In our example, pedestrians would take a point near the corner as goal and not the nearest point on the guiding line. Depending on the starting position of pedestrians, this can be far away from the corner and much longer than the shortest path to the exit.
2. The dynamical and collective influence of pedestrians: In the presence of other pedestrians and depending on the magnitude of the local density, the nature of the “quickest path” [15] changes dynamically and differs in most cases from the “shortest path” to the exit.

We therefore adopt a concept similar to ideas introduced in [16] which are well established and widely used in cellular automata models [17, 18].

At a time step t a pedestrian i heads towards a point on the line which minimizes the distance to the inner point of the corner $l^i(t)$. This is a natural territorial effect which leads to the shortest path to the exit. If all pedestrians try to take the shortest path, large jams will be observed right at the inner point of the corner. If, however, the collective influence of pedestrians dominates the choice of the desired direction, pedestrians will choose their desired direction to be orthogonal to the guiding lines and thus make better use of the whole directing line.

For this reason we include a dynamical factor that depends mainly on previous decisions taken by other pedestrians:

$$p^i(t) = \exp(-k_d \cdot \text{occ}_{\text{rel}}^i(t)), \quad (13)$$

where

$$\text{occ}_{\text{rel}}^i(t) = \frac{n^i}{n_{\text{max}}^i} \quad (14)$$

is a measure of the occupation of the line. n^i is the cardinality of the set

$$A_l = \{l^j \mid j \in B_l \text{ \& } l^j < l^i\}$$

and n_{\max}^i is the cardinality of the set

$$B_l = \{j \in [1, N] \mid i \neq j \text{ \& } \vec{e}_{i,l} \cdot \vec{e}_{i,j} \geq 0\}. \quad (15)$$

B_l is the set of all relevant neighbors of i , that influences its desired direction by means of a contribution to $\text{occ}_{\text{rel}}^i(t)$ (14). For the scenario depicted in Fig. 8 the set B_l for i (red ellipse) contains only one pedestrian j (bold ellipse).

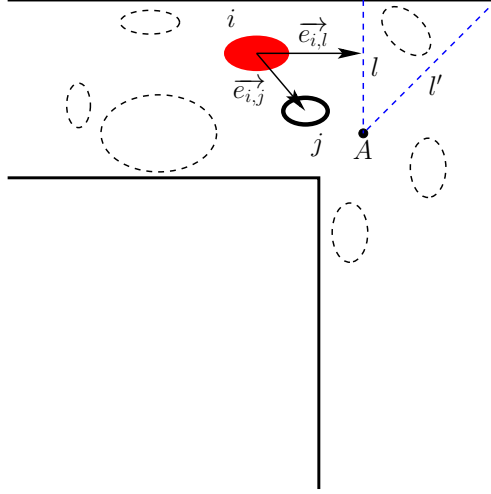


Fig. 8: How to get around the corner? Pedestrian i that is heading toward the first guiding line, considers the positions of its neighboring pedestrians as well as its initial position to decide whether or not to head closer to the edge of the corner.

Large values of $\text{occ}_{\text{rel}}^i(t)$ imply small values of $p^i(t)$. As a consequence pedestrians prefer not to change their desired direction closer to the edge of the corner.

Finally, the update rule of the distance $l^i(t)$ is given by:

$$l^i(t + \Delta t) = l^i(t) \cdot (1 - p^i(t)). \quad (16)$$

$p^i(t) \in [0, 1]$ gives the rate of change from the initial “guess” of pedestrian i . For $p^i(t) = 0$ the desired direction of i stays orthogonal to the guiding line, while $p^i(t) = 1$ displays the case where i 's desired direction is directed to the edge of the corner A . In the next section we study the influence of the parameter k_d on the dynamics of pedestrians. For the second and third line we set $k_d = 0$ and vary it only for the first line.

4 Analysis of the sensitivity parameter

To understand the impact of the collective influence of pedestrians on the chosen target point for each pedestrian i , we study the time evolution of the relative length for different values of k_d . The relative length is defined as

$$l_{\text{rel}}^i(t) = \frac{l^i(t)}{l_{\text{max}}} \quad (17)$$

where l_{max} is the length of the guiding line.

Fig. 9a shows the probability distribution of the relative length for $k_d = 0$. Pedestrians are mainly heading towards A and the full length of the directing line is rarely used.

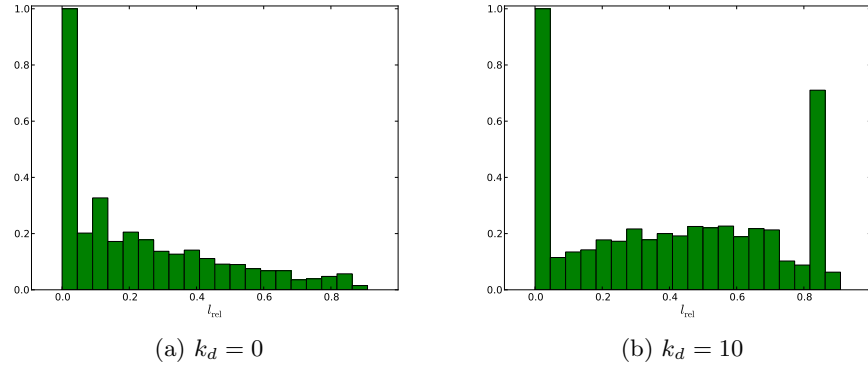


Fig. 9: Movement of $N = 100$ pedestrians around a corner with different values of k_d . The width of the corridor is $w = 3$ m.

The situation changes considerably for $k_d = 10$. Fig. 9b shows that the distribution of the length is more balanced which indicates that pedestrians make better use of the directing lines.

To showcase the impact of collective influence of pedestrians on the desired direction, we show in Fig. 10 the variation of the movement time in dependence of k_d .

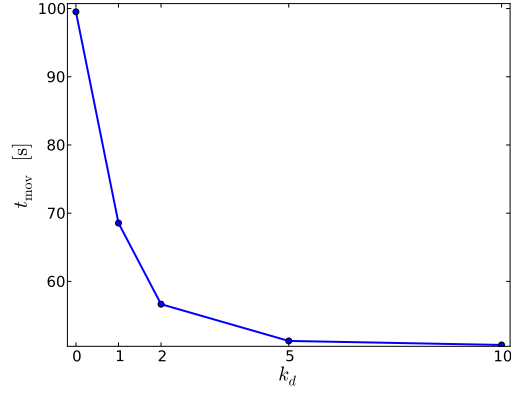


Fig. 10: Movement time for a simulation with $N = 100$ pedestrians around a corner for different values of k_d .

A qualitative comparison shown in Fig. 11 confirms the above-mentioned quantitative analysis.

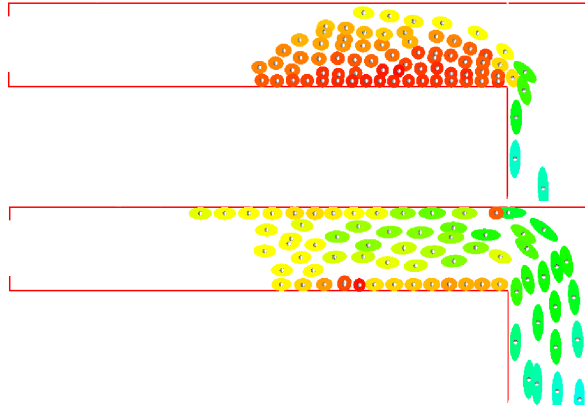


Fig. 11: Screen shot of a simulation with 100 pedestrians, $k_d = 0$ (top) and $k_d = 10$ (bottom).

For $k_d = 0$ a jam forms immediately before the corner as indicated by the large number of slowly moving pedestrians (red ellipses). This results from a strong competition between the pedestrian to pass close to the edge A of the corner. In contrast, for $k_d = 10$ pedestrians move quicker since they make optimal use of the guiding line.

5 Summary

We have developed a strategy to determine the desired direction \vec{e}_i^0 for each pedestrian i . This method is rather general and can be used in each geometry characterized by the existence of corners, e.g. bottlenecks (2 corners), T-Junction (2 corners). In analogy to CA models we introduced and tested a factor to model the static and dynamic interactions of pedestrians with the geometry.

Our work was based on an enhanced version of the GCFM [6]. The enhancements use a considerable simplification of the repulsive forces acting on pedestrians from walls. Furthermore, we addressed an important issue in force-based models, namely the choice of the desired direction of pedestrians. Several strategies were implemented and compared with empirical data. This comparative investigation showed that the outcome of a simulation depends strongly on the chosen direction of the desired direction of pedestrians. Finally, we introduced a new mechanism to direct pedestrians in 90°-corners by means of directing lines. The main concept of this strategy base on the well-known concept of dynamical floor-field. For further works, the parameter k_d that expresses the tendency of pedestrians to take the shortest path (or not) should be varied individually as the geometrical and dynamical conception of pedestrians differ.

Acknowledgments

This work is within the framework of two projects. The authors are grateful to the Deutsche Forschungsgemeinschaft (DFG) for funding the project under Grant-No. SE 1789/1-1 as well as the Federal Ministry of Education and Research (BMBF) for funding the project under Grant-No. 13N9952 and 13N9960.

References

- [1] Helbing D (1991) Behavioral Science, 36:298–310
- [2] Helbing D, Molnár P (1995) Phys. Rev. E, 51:4282–4286
- [3] Lakoba T I, Kaup D J, Finkelstein N M (2005) Simulation, 81:339–352
- [4] Yu W J, Chen L Y, Dong R, Dai S Q (2005) Phys. Rev. E, 72(2):026112
- [5] Johansson A, Helbing D, Shukla P K (2007) Adv. in Compl. Sys., 10(2):271–288
- [6] Chraïbi M, Seyfried A, Schadschneider A (2010) Phys. Rev. E, 82:046111
- [7] Steffen B, Seyfried A (2009) Modelling of Pedestrian Movement around 90° and 180° Bends. In Topping B H V, Tsompanakis Y (eds) The First International Conference on Soft Computing Technology in Civil, Structural and Environmental Engineering. Civil-Comp Press, Stirlingshire, UK

- [8] Gloor C, Maun L, Nagel K (2003) A pedestrian simulation for hiking in the alps. In Proceedings of the Swiss Transport Research Conference (STRC), Monte Verita, CH
- [9] Moussaïd M, Helbing D, Theraulaz G (2011) Proc. Nat. Acad. Sc., 108(17):6884–6888
- [10] Höcker M, Berkahn V, Kneidl A, Borrmann A, Klein W (2010) Graph-based approaches for simulating pedestrian dynamics in building models. In 8th European Conference on Product & Process Modelling (ECPPM), University College Cork, Cork, Ireland
- [11] Kemloh Wagoun A U, Seyfried A (2010) Optimizing the evacuation time of pedestrians in a graph-based navigation. In Panda M, Chattararaj U (eds) Developments in Road Transportation, Macmillian Publishers India Ltd
- [12] Kretz T, Große A, Hengst S, Kautzsch L, Pohlmann A, Vortisch P (2011) Adv. in Compl. Sys., 14(5):733–759
- [13] Molnár P (1995) Modellierung und Simulation der Dynamik von Fußgängerströmen. PhD Thesis, Universität Stuttgart, Stuttgart
- [14] Liddle J, Seyfried A, Klingsch W, Rupprecht T, Schadschneider A, Winkens A (2009) An Experimental Study of Pedestrian Congestions: Influence of Bottleneck Width and Length. In Traffic and Granular Flow 2009 (arXiv:0911.4350)
- [15] Kretz T (2009) J. Stat Mech.: Theory and Experiment, P03012
- [16] Burstedde C, Klauck K, Schadschneider A, Zittartz J (2001) Physica A, 295:507–525
- [17] Nishinari K, Kirchner A, Namazi A, Schadschneider A (2004) IEICE Transactions, 87-D(3):726–732
- [18] Kretz T, Schreckenberg M (2006) The F.A.S.T.-Model. In Lect. Notes Comp. Sc., 4173:712–715, Springer Berlin/Heidelberg